

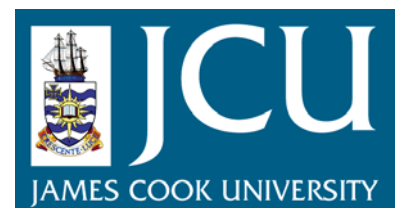
JCU ePrints

This file is part of the following reference:

Young, Ian Robert (1983) *The response of waves to an opposing wind*. PhD thesis, James Cook University.

Access to this file is available from:

<http://eprints.jcu.edu.au/12010>



THE RESPONSE OF WAVES TO
AN OPPOSING WIND

Thesis submitted by
Ian Robert YOUNG BE, MEngSc
in May 1983

for the degree of Doctor of Philosophy in
the Department of Civil and Systems Engineering at
James Cook University of North Queensland

ABSTRACT

The results of a laboratory study of the response of waves to an opposing wind are presented. The study was conducted in a special purpose wind-wave flume which allowed mechanically generated waves to propagate in opposition to wind. The mechanically generated waves were created by a wedge wave maker for which an extensive set of measurements were performed to determine its transfer function. A wave follower which could hold pressure and velocity probes a fixed distance above the moving water surface was designed and constructed. Extensive evaluation experiments indicated that the wave follower tracked the water surface with little error in the frequency range of interest. The transfer functions of all intermediate devices in the pressure and velocity recording systems were determined and subsequently used to correct all pressure and velocity records. Measurements of the wave induced pressure at various heights above the waves indicated that the pressure and water surface were 180° out of phase, consistent with the predictions of potential flow theory. Such a result indicates that there is no air-water energy flux due to normal stresses. Measurements of the velocity field above the waves indicated that the Reynolds stress term $-\rho \overline{u''u''}$ can cause waves to decay in an opposing wind. The magnitude of the decay is proportional to the wave slope squared and the term $(1 - U_\infty/C)$ squared. Hence, high frequency waves will decay far more rapidly than low frequency waves. Typical results indicate that low frequency ocean swell is almost unaffected by opposing winds whereas high frequency wind waves will be attenuated very rapidly.

TABLE OF CONTENTS

	<u>Page No.</u>
List of Tables	vi
List of Figures	vii
List of Symbols	xv
Acknowledgements	xix
1. <u>INTRODUCTION</u>	1
2. <u>ENERGY TRANSFER AT THE AIR-WATER INTERFACE</u>	3
2.1 Radiative Transfer Equation	3
2.2 Theories of Air-Water Energy Exchange	7
2.2.1 Potential Theory	7
2.2.2 Kelvin-Helmholtz Instability	10
2.2.3 Jeffreys' Sheltering Theory	12
2.2.4 The Miles-Phillips Theory	13
2.3 Wave-Wave Interactions	18
2.3.1 Resonant Interactions	18
2.3.2 Long Wave - Short Wave Interaction	21
2.4 Wave-Current Interaction	22
2.5 Wave Dissipation	24
2.5.1 The Saturation Range	24
2.5.2 Bottom Dissipation	27
2.6 Measurements of Air-Sea Interaction	29
2.6.1 Wave Growth	29
2.6.2 Opposing Winds	20
2.7 Stress at the Water Surface	31

	<u>Page No.</u>
3. <u>LABORATORY WIND-WAVE FLUME</u>	39
3.1 Laboratory Modelling and Simulation	39
3.2 Design of Wind-Wave Flume	44
3.2.1 Existing Facility	44
3.2.2 Modified Facility	47
3.2.3 Fan Design	50
3.2.4 Performance Evaluation of Air Flow	51
3.3 Wave Maker Performance	54
3.3.1 Theoretical Transfer Functions	54
3.3.2 Measured Transfer Functions	56
3.4 Wave Reflections	62
3.4.1 Reflection of Mechanically-Generated Waves from the Beach	62
3.4.2 Reflection of Wind-Generated Waves from the Wave Maker	63
3.5 Water Level Setup	64
4. <u>INSTRUMENTATION</u>	66
4.1 Water Level Measurement System	66
4.2 Water Level Follower	68
4.2.1 Wave Follower Description	68
4.2.2 Wave Follower Performance	69
4.3 Pressure Measurement System	71
4.3.1 Description of System	71
4.3.2 Pressure Transducer Calibration	73
4.3.3 Disk Pressure Probe Calibration	75
4.3.4 Calibration of Total Probe for Pitch and Yaw	76
4.3.5 The Effects of Flow Turbulence	76
4.3.6 The Dynamic Response of Pressure Tubing	77
4.3.7 Wave-Follower-Induced Pressure	81
4.3.8 Response of Electronic Systems	83

	<u>Page No.</u>
4.4 Velocity Measurement Systems	84
4.4.1 Hot Film Anemometer Systems	84
4.4.2 Probe Calibration	85
4.4.3 Probe Alignment	86
4.5 Data Acquisition and Experimental Control	87
4.5.1 Minicomputer System	87
4.5.2 Spectrum Analyser	88
5. <u>SURFACE DRIFT CURRENT</u>	89
6. <u>SPATIAL WAVE DECAY</u>	93
7. <u>SURFACE PRESSURE FIELD</u>	95
8. <u>SURFACE VELOCITY FIELD</u>	97
8.1 Boundary Layer Profiles Above Waves	97
8.2 Wave-Induced Velocities	99
8.3 Reynolds Stresses	103
9. <u>THE WIND-WAVE ENERGY FLUX</u>	109
10. <u>VISUAL OBSERVATIONS</u>	111
11. <u>COMPARISON WITH OTHER RESULTS</u>	113
12. <u>CONCLUSIONS</u>	115
APPENDIX A - Dynamic Response of Pressure Tubing	116
APPENDIX B - Error Sources in Spectral Analysis	118
APPENDIX C - Analysis of Very Narrow Band Data	121
APPENDIX D - Corrections for System Response	124
APPENDIX E - Analysis of Pressure Data	126

	<u>Page No.</u>
APPENDIX F - Test Procedure for Computer Program for Transfer Function Correction of Differential Pressure Records	130
APPENDIX G - Analysis of Velocity Data	131
APPENDIX H - Error Analysis	134
APPENDIX I - Least Squares Curve Fitting	141
APPENDIX J - Design of Digital Filters	143
APPENDIX K - Relationship Between Fixed Probe and Oscillating Probe Measurements	147a
BIBLIOGRAPHY	148

LIST OF TABLES

		<u>Page No.</u>
2.1	Components of the x, z stress tensor.	36
2.2	Energy flux directions as a function of surface stress-water surface phase difference.	38
3.1	Estimated values of wind-wave flume boundary layer thickness.	49
3.2	Estimated section loss coefficients.	51
3.3	Command signal spectral parameters.	59
3.4	Command signal variances.	59
5.1	Surface drift current versus free stream wind velocity.	89
5.2	Effect of surface drift current on wave phase speed.	91
5.3	Wave attenuation due to opposing current.	91
6.1	Theoretical viscous decay rates of waves.	94
H.1	Estimated experimental errors.	140

LIST OF FIGURES

	<u>Page No.</u>	
2.1	Wave induced pressure as predicted by potential theory.	161
2.2	Wave induced velocities as predicted by potential theory.	161
2.3	Example of rotational flow.	162
2.4	Theoretical wave growth and decay [after Phillips (93)].	163
2.5	The energy transfer due to wave-wave interactions for the JONSWAP spectrum.	164
2.6	Wave response to a current.	162
2.7	Measurements of the pressure-water surface phase shift in a following wind.	165
2.8	Measurements of air-sea energy flux in a following wind.	166
2.9	Wave decay in an opposing wind [after Stewart and Teague (124)].	166
2.10	Definition diagram of stress at the water surface.	169
3.1	Plan of existing wave flume.	167
3.2	Photograph of existing wave flume	168
3.3	Diagram of wave absorbing beach.	169
3.4	Photograph of wedge wave maker.	170
3.5	The wave maker control system.	171
3.6	Diagram of wedge wave maker	172

	<u>Page No.</u>
3.7 Plan of fan, motor and power transmission assembly.	179
3.8 Diagram of complete wind-wave flume.	173
3.9 Fan-flume load characteristic curve.	175
3.10 Mean velocity profile at flume inlet.	176
3.11 Vertical profile of turbulent intensities at flume inlet.	176
3.12 Spectrum of longitudinal turbulence in the air at flume inlet.	177
3.13 Cross-section velocity contours at flume inlet and working section.	178
3.14 Free stream wind velocity as a function of fan speed.	179
3.15 Time series of water surface elevation produced by a sinusoidal wave maker motion.	180
3.16 Spectra of water surface elevation produced by a sinusoidal wave maker motion.	181
3.17 Schematic diagram of individual influences in wave-maker transfer function.	183
3.18 Transfer function relating command signal and wave maker motion.	184
3.19 Transfer functions relating command signal and water surface elevation at mid-flume.	185
3.20 Typical command signal-water surface elevation phase relationship.	188
3.21 Average transfer function relating command signal and water surface elevation at mid flume.	189

	<u>Page No.</u>
3.22 Theoretical transfer function relating wave maker and water surface elevation.	189
3.23 Theoretical transfer function relating command signal and water surface elevation.	190
3.24 Average transfer function relating command signal and water surface elevation at beach.	190
3.25 Test of wave maker transfer function.	191
3.26 Spectrum of wind waves with and without wave dissipater at wave maker end.	192
3.27 Water level setup in flume.	193
4.1 Photograph of resistance wave gauge.	194
4.2 Schematic diagram of wave gauge system.	195
4.3 Circuit diagram of wave gauge bridge and isolation transformers.	196
4.4 Wave gauge calibration and mounting system.	196
4.5 Typical wave gauge calibration curve.	197
4.6 Test of wave gauge stability with time.	197
4.7 Diagram of wave follower.	198
4.8 Photograph of wave follower.	199
4.9 Comparison of spectra of water surface elevation and wave follower position.	200

	<u>Page No.</u>
4.10 Transfer function relating water surface elevation and wave follower position.	201
4.11 Coherence function between water surface elevation and wave follower position.	202
4.12 Spectrum of "hunting" wave follower in still water.	202
4.13 Schematic diagram of pressure measurement system.	203
4.14 Dimensions of disk pressure probe.	204
4.15 Photograph of pressure probes.	205
4.16 Schematic diagram of pressure recording system.	204
4.17 Photograph of calibration wind tunnel.	206
4.18 Schematic diagram of pressure transducer calibration system.	207
4.19 Typical pressure transducer calibration curve.	208
4.20 Calibration curve for disk pressure probe.	209
4.21 Response of disk probe to pitch and yaw.	210
4.22 Response of total probe to pitch and yaw.	210
4.23 Theoretical transfer function for pressure tubing.	211
4.24 Photograph of dynamic pressure generating system.	213
4.25 Measured transfer functions for the various pressure tubes.	214

	<u>Page No.</u>	
4.26	Transfer functions for the wave follower induced pressures.	218
4.27	Phase of the difference of two sinusoidal signals.	220
4.28	Transfer functions of the 5 Hz low pass filters.	221
4.29	Mounting system for hot film probe.	220
4.30	Typical hot film calibration curve.	223
4.31	Hot film cooling laws.	223
4.32	Photograph of spectrum analyser and other instrumentation.	224
5.1	Surface drift current as a function of free stream wind velocity.	225
6.1	Spatial wave decay as a function of U_{∞}/C .	225
7.1	Time series of water surface elevation and wave-induced pressure for various wind velocities.	226
7.2	Phase angle between \tilde{p} and η as a function of U_{∞}/C .	231
7.3	Measured values of \tilde{p} as a function of the potential flow prediction.	231
8.1	Mean velocity profiles for various f and U_{∞} .	232
8.2	Shear velocity, u_* as a function of U_{∞} for various f .	238
8.3	Comparison of u_* values with data from following wind experiments.	238
8.4	Time series of water surface elevation and wind velocities in the x and z directions.	239

	<u>Page No.</u>
8.5 Phase angle between \tilde{u} and η as a function of U_∞/C (stationary probe).	245
8.6 Phase angle between \tilde{w} and η as a function of U_∞/C (stationary probe).	245
8.7 $\text{amp}(\tilde{u})$ as a function of a potential flow prediction (stationary probe).	246
8.8 $\text{amp}(\tilde{w})$ as a function of the potential flow prediction (stationary probe).	246
8.9 Phase angle between \tilde{u} and η as a function of U_∞/C (wave following probe).	247
8.10 Phase angle between \tilde{w} and η as a function of U_∞/C (wave following probe).	247
8.11 $\text{amp}(\tilde{u})$ as a function of the potential flow prediction (wave following probe).	248
8.12 $\text{amp}(\tilde{w})$ as a function of the potential flow prediction (wave following probe).	248
8.13 Wave induced velocities recorded with a following wind.	249
8.14 Spectra of u'' and w'' , coherence between u'' and w'' and phase angle between u'' and w'' for $f = 1$ Hz and various values of z .	250
8.15 $\overline{u''u''}$ as a function of the wave-induced Reynolds stress predicted by potential theory (stationary probe).	256
8.16 $\overline{w''w''}$ as a function of the wave-induced Reynolds stress predicted by potential theory (stationary probe).	256

	<u>Page No.</u>
8.17 $\overline{u''w''}$ as a function of the potential flow wave-induced velocity squared (stationary probe).	257
8.18 $\overline{u''u''}$ as a function of the wave-induced Reynolds stress predicted by potential theory (wave following probe).	257
8.19 $\overline{w''w''}$ as a function of the wave-induced Reynolds stress predicted by potential theory (wave following probe).	258
8.20 $\overline{u''w''}$ as a function of the potential flow wave-induced velocity squared (wave following probe).	258
8.21 $\overline{u''w''}$ as a function of U_∞^2 (wave following probe).	259
8.22 Spectra of $u''u''$, $w''w''$ and $u''w''$.	260
9.1 Air-sea energy flux in an opposing wind.	263
9.2 Wave decay as a function of fetch and duration for various ak and U_∞ .	264
10.1 Photographs of waves in an opposing wind.	268
A.1 Definition sketch of pressure tube system of Bergh and Tjrdeman (6).	274
B.1 Fourier transforms of common window functions.	275
C.1 Spectra of sinusoidal signals of various length.	276
C.2 Crosscorrelograms of signals with various phase differences.	277
D.1 Folding of the Fourier transform about the Nyquist frequency.	278
D.2 Test of transfer function correction program.	279

	<u>Page No.</u>
E.1 Schematic diagram of system effects on pressure measurements.	280
E.2 Definition sketch of applied and measured pressures for the pressure tube system.	274
F.1 Test of computer program TUBTRN.FOR.	281
G.1 Schematic diagram of velocity measurement system.	282
J.1 Transfer functions for ideal low pass, band pass and band reject filters.	283
J.2 Transfer function for digital low pass filter for various numbers of filter weights.	284
J.3 Transfer function for digital band pass filter.	288
J.4 Transfer function for digital band reject filter.	289

LIST OF SYMBOLS

<u>Symbol</u>	<u>Definition</u>	<u>Dimension</u>
a	wave amplitude	L
\bar{A}	mean of quantity A	-
\tilde{A}	wave-induced component of A	-
A'	turbulent component of A	-
A''	fluctuating component of A	-
C	phase speed	LT^{-1}
C_f	friction factor	-
C_g	group velocity	LT^{-1}
C_I	interfacial wave speed	LT^{-1}
d	water depth	L
D_j	coupling coefficient	-
$E(f, \theta)$	variance spectrum	L^2T
E_c	Eckart number	-
E_∞	saturation spectrum	L^2T
f	frequency	T^{-1}
f_N	Nyquist frequency	T^{-1}
$F(\underline{k})$	variance spectrum	L^4
g	gravitational acceleration	LT^{-2}
H	complex transfer function	-
i	complex operator = $\sqrt{-1}$	-
\underline{k}	wave number vector	L^{-1}
K	disk probe calibration constant	-
Lr	scale length ratio	-
n	model scale	-
N	complex frequency	radians
p	pressure	$ML^{-1}T^{-2}$
p_D	disk probe pressure	$ML^{-1}T^{-2}$

<u>Symbol</u>	<u>Definition</u>	<u>Dimension</u>
p_s	static pressure	$ML^{-1}T^{-2}$
p_{so}	free stream static pressure	$ML^{-1}T^{-2}$
p_t	total probe pressure	$ML^{-1}T^{-2}$
Pr	Prandtl number	-
Q	source term	L^4T^{-1}
Re	Reynolds number	-
Ri	Richardson number	-
Ro	Rosby number	-
R_s	radiation stress	$ML^{-1}T^{-2}$
$R_x(\tau)$	autocorrelation function	L^2
$R_{xy}(\tau)$	crosscorrelation function	L^2
s	Jeffrey's sheltering coefficient	-
S	source term	L^2
S_A	air-sea interaction source term	L^2
S_D	dissipation source term	L^2
S_N	wave-wave interaction source term	L^2
t	time	T
T	surface tension	$ML^{-1}T^{-2}$
T	temperature	degrees C
Tr	scale time ratio	-
u	instantaneous x velocity	LT^{-1}
u_c	surface drift current velocity	LT^{-1}
u_i	instantaneous velocity in i direction	LT^{-1}
$u_T(t)$	window function	-
u_*	shear velocity	LT^{-1}
U	mean wind velocity	LT^{-1}
U_a	wind velocity at height a	LT^{-1}
U_∞	mean wind velocity outside boundary layer	LT^{-1}

<u>Symbol</u>	<u>Definition</u>	<u>Dimension</u>
v	general velocity	LT^{-1}
V	volume	L^3
V_r	scale velocity ratio	-
w	instantaneous z velocity	LT^{-1}
x	horizontal cartesian coordinate	L
$x(t)$	input time series	-
y	horizontal cartesian coordinate	L
$y(t)$	output time series	-
z	vertical cartesian coordinate	L
z_c	height of critical layer	L
z_g	gradient height	L
z_o	roughness scale length	L
α	angle	degrees
α	power law exponent	-
$\gamma^2(f)$	coherence function	-
δ	boundary layer thickness	L
η	water surface elevation	L
θ	angle	degrees
κ	von Karman's constant	-
μ	coupling coefficient	-
μ	dynamic viscosity	$ML^{-1}T^{-1}$
ν	coupling coefficient	-
$\pi(k, \omega)$	atmospheric pressure spectrum	$M^2L^{-2}T^{-3}$
ρ_a	air density	ML^{-3}
ρ_w	water density	ML^{-3}
σ	normal stress	$ML^{-1}T^{-2}$
τ	shear stress	$ML^{-1}T^{-2}$
ϕ	phase angle	degrees

<u>Symbol</u>	<u>Definition</u>	<u>Dimension</u>
ϕ	velocity potential function	L
χ^2	chi-squared distribution	-
ψ	angle of hot film to fluid flow	degrees
ω	frequency	radians
ω_0	wave frequency in absence of current	radians

ACKNOWLEDGEMENTS

I wish to express my gratitude to my supervisor, Dr. R.J. Sobey whose continual encouragement and significant assistance has been invaluable. It has been a considerable pleasure to work with him.

The typing of this manuscript has been executed by Mrs. Heather Stephens whose patience and diligence is much appreciated.

The wave flume and much of the instrumentation was constructed by Mr. Curt Arrowsmith and Mr. Bill Deacon and the electronics by Mr. Reg Mercer and Mr. Alf Coleman.

The project was supported financially by Woodside Offshore Petroleum Pty. Ltd. and for the duration of the project the author was employed by the James Cook University of North Queensland.

The project was conducted within the Department of Civil and Systems Engineering and I wish to thank the Head of Department, Professor K.P. Stark for his continual encouragement and interest.